This article has been accepted for publication in a future issue of this journal, but has not been fully edited. Content may change prior to final publication. Citation information: DOI 10.1109/LAWP.2019.2950369, IEEE Antennas and Wireless Propagation Letters

A Wideband and Low Side Lobe Series Fed Patch Array at 5.8 GHz for Radar Applications

G. Sacco, *Student Member, IEEE*, P. D'Atanasio, and S. Pisa, *Senior Member, IEEE*

***Abstract*—In this paper a novel series fed patch array working in the $5.8\,\mathrm{GHz}$ ISM band for healthcare radar monitoring applications has been proposed. The single patch has been opportunely shaped to solve two critical problems of this antenna topology: reduced bandwidth and high Side Lobe Level (SLL). The bandwidth enhancement has been obtained with a dual band structure, resulting from the superposition of two tapered patches with different lengths. For the side lobes, a non conventional technique, based on the modulation of the power transferred by one patch to the following one has been proposed. An electrical two port model of the single patch has been developed to significantly speed up the design process of longer series fed arrays. The model impedance matrix shows a good agreement with the one extracted from electromagnetic simulations. The designed antenna shows a fractional bandwidth of 5.92% (more than twice the available one at $5.8\,\mathrm{GHz}$) and a SLL of about $-20\,\mathrm{dB}$ inside all the bandwidth. A prototype has been realized and both reflection coefficient and radiation pattern at $5.8\,\mathrm{GHz}$ have been measured showing an excellent agreement with simulation results.**

***Index Terms*—low side lobes, patch antenna, series fed array, wideband.**

I. Introduction

Life expectancy is increasing worldwide resulting in a growing need for novel assistive technologies for non-invasive long-term home monitoring. For this kind of applications, radar sensors have shown several advantages over other alternatives [1]–[3]. Recent works [4], [5] demonstrate that an Frequency Modulated Continuous Wave (FMCW) radar is able to contextually estimate the patient's position and their breathing rate. Considering that maximum breast excursions during spontaneous respiration are about $1.5\,\mathrm{cm}$ [6], the ISM band centred at $5.8\,\mathrm{GHz}$, having a free space wavelength of about $5\,\mathrm{cm}$, is a good candidate for breath detection. Regarding instead the position estimation, since the radar resolution is inversely proportional to the bandwidth [7], it is crucial to use antennas with a band equal or larger than the available one. Another important parameter in these kind of monitoring systems is the antenna Side Lobe Level (SLL), that must be as low as possible to increase the detection performance. To reach these features, various types of microstrip antennas have been proposed [8]–[11]. In particular, series fed arrays represent a compact and low cost solution. However, these antennas show a non negligible SLL and suffer from a reduced bandwidth, a significant issue in the $5.8\,\mathrm{GHz}$ ISM frequency range, in which the allowed fractional bandwidth is about 2.6%. In the recent years numerous efforts have been devoted to broadening the bandwidth of this kind of antennas and to reducing the SLL. For the SLL, different configurations concerning the amplitude tapering of the array elements have been investigated [8], [9]. Regarding the bandwidth, solutions have been proposed, involving stacked and complex structures [10] or hybrid series-corporate feed techniques [11] requiring a larger antenna area occupation. In this work the possibility to design a wideband and low side lobes series fed array leveraging solely on modifications of the patch shape is studied in depth. The proposed solution allows for an efficient radiating element which is compact, easy to fabricate and low cost. In addition, a non-conventional approach to lower the SLL based on the modulation of the power transferred between consecutive patches and relying on shape variation of the patch upper edge has also been investigated. Our analysis has been further enhanced with the development of a two port electrical model of the elementary patch, as an useful instrument for the reduction of the time required for the design of the whole array.

G. Sacco and S. Pisa are with the Department of Information Engineering, Electronics and Telecommunication, Sapienza University of Rome, Rome 00184, Italy (e-mail:, giulia.sacco@uniroma1.it; stefano.pisa@uniroma1.it).

P. D'Atanasio is with the Italian National Agency for New Technologies, Energy and Sustainable Economic Development, Casaccia Research Centre, Rome 00123, Italy (e-mail:,paolo.datanasio@enea.it).

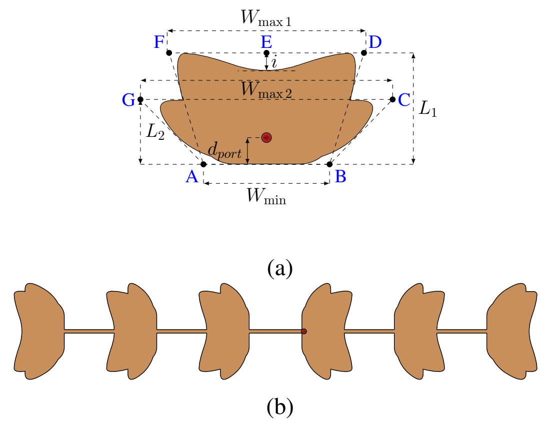

Fig. 1: (**a**) Single patch and (**b**) completed designed antenna.

II. Antenna Geometry

The antenna presented in this paper is a series fed microstrip array with a novel patch geometry, specifically designed for increasing the bandwidth and reducing the SLL. The proposed patch geometry and the complete antenna are reported in Fig. 1. The elementary radiating patch is obtained by the superposition of two tapered patches whose borders are obtained by spline interpolation respectively within the polygon $ABCG$ and $ABDEF$ of Fig. 1a. The two different lengths L_1 and L_2 introduce two resonances, while the tapering widens the bandwidth of each resonance. Another important parameter of

This article has been accepted for publication in a future issue of this journal, but has not been fully edited. Content may change prior to final publication. Citation information: DOI 10.1109/LAWP.2019.2950369, IEEE Antennas and Wireless Propagation Letters

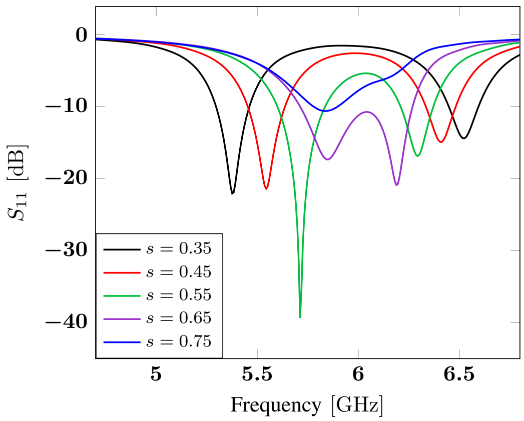

Fig. 2: Reflection coefficient of the single patch as a function of frequency for different overlapping values s.

the structure is represented by the indent i, which controls the curvature of the upper edge, with a length W_{max1}. The power transferred from one patch to the following one can be controlled by varying this last value and can hence be used to control the SLL. The complete antenna (Fig. 1b) is composed of 6 identical patches separated by microstrip lines with a length equal to half a wavelength in the dielectric. It has been designed to be fed with a coaxial connector, with the central pin directly connected to the central patch (red dot in Fig. 1b). The distance between the feed point and the patch edge (d_{port} in Fig. 1a) allows for an accurate regulation of the structure's input impedance. The array has been designed on a substrate of RO4003C [12] with a thickness h of $1.524\,\text{mm}$ and a design dielectric constant ε_r of 3.55. This thick substrate has been chosen to assure a larger bandwidth [13].

III. Antenna Design

In this section, the effects of the different patch parameters are analysed, with a particular attention given to the bandwidth enhancement and the SLL reduction.

A. Bandwidth Enhancement

To increase the bandwidth, a dual band structure has been considered. The two resonances are related to the lengths L_1 and L_2 and they can be made closer or more distant by varying the degree of superposition $s = L_2/L_1$. A first set of simulations has been performed considering a single patch, fed with a discrete port positioned at a distance $d_{port} = 0\,\text{mm}$. Fig. 2 shows the reflection coefficient for different values of superposition s and for $L_1 = 13.6\,\text{mm}$. When s is small patches are very different and the two resonances are separated, while, increasing the overlapping degree s, resonances approach until the complete overlap. By choosing the proper value of s (here $s = 0.65$) the antenna bandwidth can be increased by a factor greater than 2.

B. Side Lobe Level Reduction

The parameter that allows to control the SLL is the indent degree i. To better understand the effect of i on the SLL, the geometry represented in Fig. 3a has been considered. A patch with an overlapping degree $s = 65\%$ is fed at the lower edge and is connected with a $\lambda/2$ line to a matched load. The dielectric conductivity has been set to zero and the copper has been replaced with a Perfect Electric Conductor (PEC) to avoid substrate and metal losses. Assuming that the accepted power at the feeding port is P_a, a portion P_{Rad} of this power will be radiated and the remaining P_T will be transmitted to the next antenna elements. According to the simulated geometry, the power transmitted is identified with the one dissipated into the load. The specific amplitude distribution and correspondingly the side lobe suppression can then be controlled by indent degree i. The parameter i has been varied in the range $0\,\text{mm}-3\,\text{mm}$. Fig. 3b reports the transmitted and the radiated power normalised to the accepted one at $5.8\,\text{GHz}$. From Fig. 3b it results that, for higher i values, the radiated power increases and the transmitted one decreases. With the proposed solution, an array of identical radiating elements, with an appropriate indent degree i, fed at the edge of one of the central patches can realise a SLL control. In fact, it will give rise to a stronger radiation from the central patches and a lower one from the most external ones. It is worth noting that the effect of i is not only limited to the control of the side lobe level. In fact, when i increases, the overall patch length (L_1) is reduced and the corresponding resonant frequency is increased. Fig. 4 reports the two resonant frequencies of the single patch for different values of overlapping s and indent i. For a given value of s, when i is increased, the upper frequency value remains almost constant while the lower one increases. The results shown in Fig. 4 demonstrate that for the design of the antenna it is not possible to identify the correct values of s and i independently and that their effects cannot be separated.

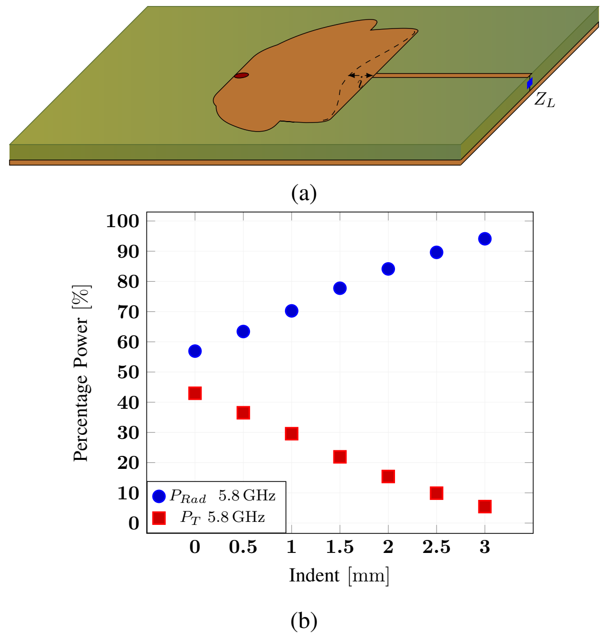

Fig. 3: (**a**) Geometry of the simulated structure for the power transfer study and (**b**) radiated and transmitted power for different values of indent at $5.8\,\text{GHz}$.

This article has been accepted for publication in a future issue of this journal, but has not been fully edited. Content may change prior to final publication. Citation information: DOI 10.1109/LAWP.2019.2950369, IEEE Antennas and Wireless Propagation Letters

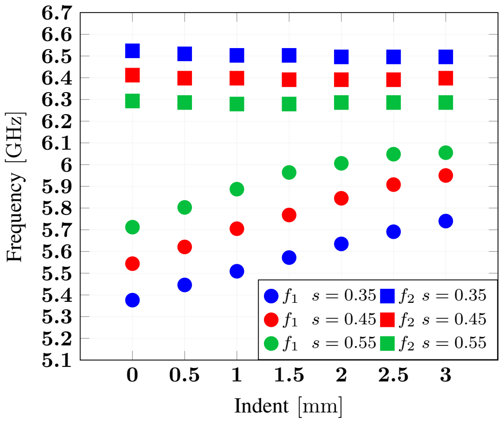

Fig. 4: Resonant frequencies for different values of s and i.

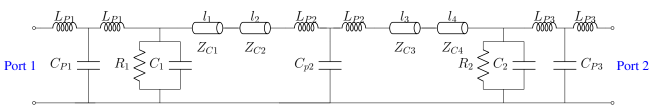

Fig. 5: Two port electrical model of the proposed patch.

IV. Equivalent Electrical Model

To simplify the design procedure of a series array, a two port electrical model of the proposed patch has been developed (Fig. 5). The model is derived from the rectangular patch transmission line model [13], but has been opportunely modified to describe the considered geometry. An array composed of multiple patches can be modelled with the cascade of multiple circuits such as the one in Fig. 5, interconnected by transmission lines with the same electrical length and characteristic impedance of the chosen microstrip lines. In particular, two T networks, realised with L_{p1} and C_{p1} at the port 1 and L_{p3} and C_{p3} at the port 2, have been added to take into consideration the discontinuities between the patch and the lines. Looking at the patch geometry (Fig. 1), two tapered sections can be clearly identified: the first one starting at the feed point and with a L_2 length and the second one starting at L_2 and extending till the end of the patch. The gradually increasing patch width of each of these two sections has been modelled by cascading two transmission lines with decreasing characteristic impedance. The lengths and the characteristic impedances of the lines are l_1 l_2, Z_1 and Z_2 for the first section and l_3, l_4, Z_3 and Z_4 for the second one. R_1, C_1 and R_2, C_2 describe the radiating slots associated with the patch and the two parasitic inductances L_{p2} and the capacitor C_{p2} take into account the current pattern variation at the distance L_2 from the feeding edge. The comparison between the Z parameter matrix obtained with the proposed model and that obtained from CST Microwave Studio simulations for a single patch are reported in Fig. 6a. The superscripts m and s have been used to distinguish model and simulation results. For the model the following values have been used: $L_{P1} = 0.16\,\text{pH}$, $C_{P1} = 1\,\text{fF}$, $R_1 = 450\,\Omega$, $C_1 = 10.01\,\text{fF}$, $Z_{c1} = 13\,\Omega$, $l_1 = 56.13\,\text{deg}$, $Z_{c2} = 6.50\,\Omega$, $l_2 = 60.13\,\text{deg}$, $C_{p2} = 39.37\,\text{pF}$, $L_{P2} = 8.00\,\text{pH}$, $Z_{c3} = 14.50\,\Omega$, $l_3 = 25.72\,\text{deg}$, $Z_{c4} = 7\,\Omega$, $l_4 = 24.42\,\text{deg}$, $R_2 = 165.10\,\Omega$, $C_2 = 0.70\,\text{pF}$, $L_{P3} = 0.17\,\text{nH}$ and $C_{P3} = 30.59\,\text{pF}$. To describe a complete array, 6 model units have been cascaded together and a $50\,\Omega$ port has been connected to the input edge of the central element. An inductance of $1.05\,\text{nH}$ has then been added to represent the feed connection effect. In Fig. 6b the real and imaginary parts of the input impedance of the structure simulated with CST and of the model are compared. Both the curves obtained with the model follow quite well the simulation results. Despite the geometry complexity, the model describes well the electromagnetic behaviour of the structure, and is a good instrument for the antenna design process.

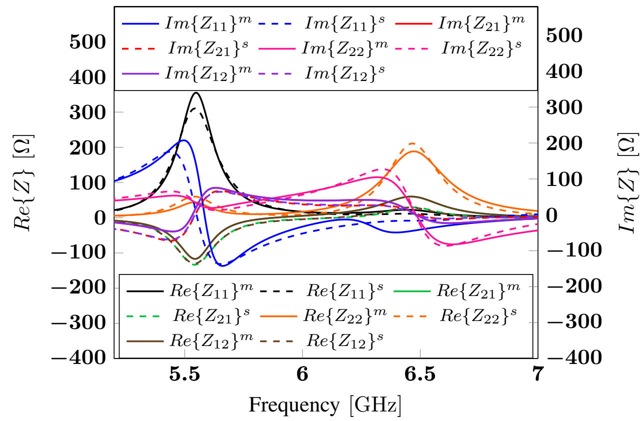

(a)

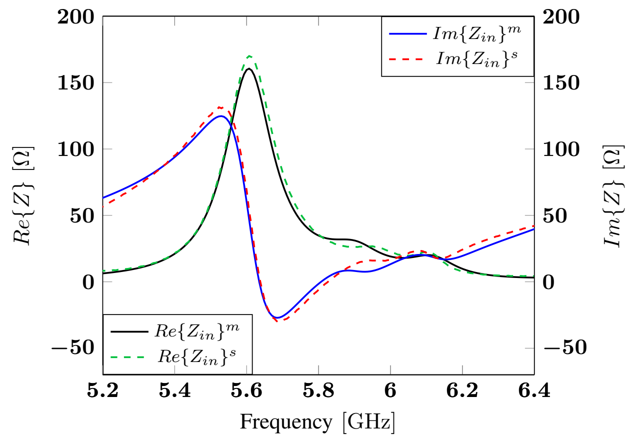

(b)

Fig. 6: Comparison between the simulated Z parameters and the ones obtained with the equivalent electrical model (**a**) for the single patch and (**b**) the complete array.

V. Realisation, Measurements and Results

A prototype of the designed six patch array has been realised with a computer numerical control (CNC) Milling Machine. The measured reflection coefficient is reported in Fig. 7 together with the simulation results. The figure shows a quite good superposition between simulations and measurements (Fig. 7). The S_{11} magnitude indicates that the structure is well matched in $343.29\,\text{MHz}$ around the central frequency $5.8\,\text{GHz}$. The corresponding fractional bandwidth is of 5.92%, which is more than the double of the 2.6% required. Further measurements have been performed inside a semi-anechoic

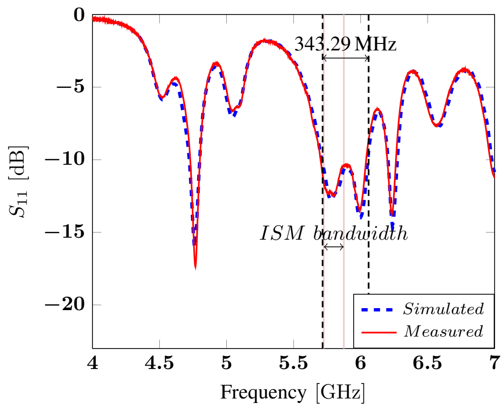

Fig. 7: Simulated and measured S_{11} of the 6 patch array.

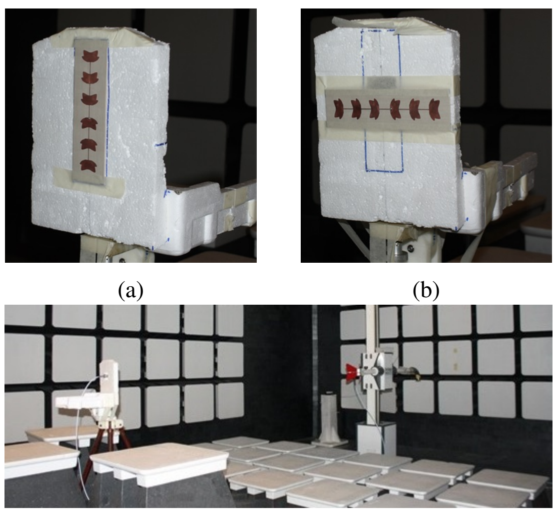

(a) (b)

(c)

Fig. 8: Picture of: (**a**) antenna support for the H-plane and (**b**) E-plane measurements and (**c**) anechoic chamber set-up.

chamber turned into a fully anechoic one by opportunely placing panels covered by ferrite tiles and pyramidal absorbers on the metallic floor. The experimental set-up is reported in Fig. 8c. The antenna under test is mounted on a dielectric easel and supported by a polystyrene structure (Fig. 8a and 8b). Both the E and H planes patterns have been tested. Measurements have been performed using the ETS-Lindgren's Model 3117 Double-ridged Waveguide antenna [14] working in the $1-18$ GHz range, that covers the ISM band at 5.8 GHz. The chosen distance between the antenna under test and the measuring one is of 2.58 m, guaranteeing the far field condition for both antennas. Measured and simulated radiation patterns are plotted in Fig. 9 both for the E and the H planes. A detailed analysis of the far field behaviour of the realised antenna compared to the simulated one is reported in Table I, with reference to the E-plane. The obtained results show a very good agreement between measurements and simulations. It is worth noting that the reduction of the SLL causes a widening of the main beam, similarly to what happens for the patch amplitude tapering. Table II reports a comparison of the proposed series fed array with the ones found in literature

TABLE I: Simulated and measured radiation characteristics of the 6 patches array (E-plane).

Frequency(GHz)	Gain (dB)		Angular width at 3 dB (°)		Side lobe level (dB)	
	Sim.	Meas.	Sim.	Meas.	Sim.	Meas.
5.725	13.9	14.5	20.0	20.5	−19.8	−20.3
5.750	14.0	14.3	19.7	21.0	−20.0	−19.2
5.775	14.1	14.6	19.3	20.0	−20.3	−19.3
5.800	14.2	14.3	19.0	20.0	−20.7	−21.6
5.825	14.2	14.7	18.6	20.0	−21.1	−19.4
5.850	14.3	14.5	18.1	20.0	−21.6	−20.8
5.875	14.3	13.3	17.7	19.5	−22.3	−21.2

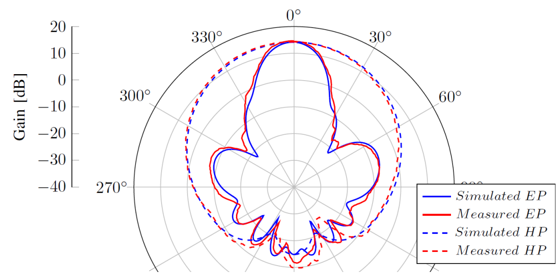

Fig. 9: Simulated and measured far field of the 6 patches series fed array at 5.8 GHz in E-Plane (EP) and H-plane (HP).

and designed in the same band, showing that the presented antenna is the one with the widest bandwidth still maintaining a low SLL.

VI. Conclusions

In this paper a novel series fed patch array working in the 5.8 GHz ISM band for radar healthcare monitoring applications has been designed. The patches have been opportunely shaped to increase the narrow bandwidth typical of rectangular patches and to lower the SLL. The bandwidth enhancement has been obtained with a dual band structure, realised by the superposition of two tapered patches with different lengths. For the SLL, a new technique, based on the modulation of the power transferred by one patch to the following one has been proposed. With this solution, with the only variation of the shape of the upper patch edge, an array with all the elements equal to each other can be designed, guaranteeing a low SLL. The performed study has been enriched by the development of a two port electrical model of the single patch. The model, which also includes the effect of the discontinuity between the patch and the feeding lines, can reach a really good agreement with electromagnetic simulations. A 6 patch array has been designed, showing a fractional bandwidth of 5.92% (more than twice the available one at 5.8 GHz) and a SLL of about -20 dB inside all the bandwidth. A prototype has been realised with a CNC Milling Machine. The reflection coefficient and the radiation pattern at 5.8 GHz have been measured showing an excellent agreement between measurements and simulation results.

TABLE II: Comparison of the proposed array with literature.

Ref	Bandwidth (MHz)	Side lobe level (dB)
[8]	140 MHz	−14 dB
[9] Array 1	60 MHz	−14.5 dB
[9] Array 2	75 MHz	−28.6 dB
Proposed	340 MHz	−22.3 dB

REFERENCES

[1] S. Pisa, E. Pittella, and E. Piuzzi, "A survey of radar systems for medical applications," *IEEE Aerospace and Electronic Systems Magazine*, vol. 31, no. 11, pp. 64–81, Jul. 2016.

[2] C. Li, V. M. Lubecke, O. Boric-Lubecke, and J. Lin, "A review on recent advances in Doppler radar sensors for noncontact healthcare monitoring," *IEEE Transactions on microwave theory and techniques*, vol. 61, no. 5, pp. 2046–2060, May 2013.

[3] C. Li, Z. Peng, T.-Y. Huang, T. Fan, F.-K. Wang, T.-S. Horng, J.-M. Muñoz-Ferreras, R. Gómez-García, L. Ran, and J. Lin, "A review on recent progress of portable short-range noncontact microwave radar systems," *IEEE Transactions on Microwave Theory and Techniques*, vol. 65, no. 5, pp. 1692–1706, May 2017.

[4] G. Sacco, E. Pittella, E. Piuzzi, and S. Pisa, "A radar system for indoor human localization and breath monitoring," in *2018 IEEE International Symposium on Medical Measurements and Applications (MeMeA)*. IEEE, Jun. 2018, pp. 1–6.

[5] M. Mercuri, I. R. Lorato, Y.-H. Liu, F. Wieringa, C. Van Hoof, and T. Torfs, "Vital-sign monitoring and spatial tracking of multiple people using a contactless radar-based sensor," *Nature Electronics*, p. 1, Jun. 2019.

[6] O. Boric-Lubecke, V. M. Lubecke, A. D. Droitcour, B.-K. Park, and A. Singh, *Doppler radar physiological sensing*. Wiley Online Library, Jan. 2016.

[7] C. Li, M.-R. Tofighi, D. Schreurs, and T.-S. J. Horng, *Principles and Applications of RF/microwave in Healthcare and Biosensing*. Academic Press, Oct. 2016.

[8] T. Yuan, N. Yuan, and L.-W. Li, "A novel series-fed taper antenna array design," *IEEE antennas and wireless propagation letters*, vol. 7, pp. 362–365, Oct. 2008.

[9] R. Chopra and G. Kumar, "Series-fed binomial microstrip arrays for extremely low sidelobe level," *IEEE Transactions on Antennas and Propagation*, vol. 67, no. 6, pp. 4275–4279, Mar. 2019.

[10] X. Zhang, J. Huyan, P. Gao, H. Wang, and Y. Zheng, "Stacked series-fed linear array antenna with reduced sidelobe," *Electronics Letters*, vol. 50, no. 4, pp. 251–253, Feb. 2014.

[11] W. Yang, K. Ma, K. S. Yeo, and W. M. Lim, "A compact high-performance patch antenna array for 60-ghz applications," *IEEE Antennas and Wireless Propagation Letters*, vol. 15, pp. 313–316, Jun. 2015.

[12] "Ro4000®series high frequency circuit materials," Rogers Corporation, 2018.

[13] C. Balanis, *Antenna theory: analysis and design*, ser. Harper & Row series in electrical engineering. Wiley, Feb. 2016.

[14] "Double-ridged guide 3117 double-ridged guide antenna," ETS-Lindgren, Mar. 2014.